Available online at www.sciencedirect.com
SCIENCE DIRECT®
Journal of Pharmaceutical and Biomedical Analysis
33 (2003) 891–901
JOURNAL OF PHARMACEUTICAL AND BIOMEDICAL ANALYSIS
www.elsevier.com/locate/jpba

Comparison between mono- and bi-exponential models for reaction kinetics in the immunoradiometric assay of neuron-specific enolase

J. García Gómez, J.L. Moreno Frigols *

Department of Physical Chemistry, Valencia Pharmacy Faculty, Radioisotope Service, Valencia University Hospital, Avda. Vicent Andrés Estellés s/n, 46110 Burjassot (Valencia), Spain

Received 12 March 2003; received in revised form 25 June 2003; accepted 25 June 2003

Abstract

This paper studies the kinetics of the antigen–antibody reactions involved in the analytical determination of neuron-specific enolase (NSE) by means of radiometric immunoassay (IRMA). For the global process, kinetics were found to be dependent on analyte and labelled antibody concentrations, such dependence fitting with the models described in previous papers [1,2]. Viscosity results clearly indicate its negative influence on the direct reaction rate. Ionic strength shows noticeable but not too relevant effects, which suggests that the variation caused by the glycerol addition is not due to the influence of the dielectric constant of the solutions used. The effect of temperature shows activation parameters similar to the viscous flow energy of water, which suggests diffusion control for the global process. The analysis of the kinetic data of the experiences conducted can be explained by admitting that the antigen–antibody binding takes place through two different binding site types.

Keywords: Immunoradiometric assay; Neuron-specific enolase; Viscosity; Ionic strength; Temperature; Diffusion; Binding sites

1. Introduction

Enolase (phosphopyruvate hidratase, 2-phospho-D-glicerate hydro-lyase, E.C.4.2.1.11) is an enzyme involved in the metabolism of glucose. Enolase is present in all cells in higher animals.

The Enolase molecule is composed of two subunits. Three different types of subunits, termed α, β, and γ, have been described. The γ unit is found either in a homologous γ–γ or in a heterologous α–γ isoenzyme. Both types mainly occur in nerve cells or neurorktodermal cells, and are collectively known as neuron-specific enolase (NSE). Recent investigation has shown that NSE is not absolutely specific for nerve cells or neuroektodermal cells, but is also present, although in much smaller quantities, in cells of other origin.

Quantitative determination of NSE in serum is valuable in the management of patients with

* Corresponding author. Tel.: +34-96-354-4894; fax: +34-96-354-4892.
E-mail address: jose.l.moreno@uv.es (J.L. Moreno Frigols).

0731-7085/03/$ - see front matter © 2003 Elsevier B.V. All rights reserved.
doi:10.1016/S0731-7085(03)00418-7

suspected or diagnosed neuroblastoma and small lung carcinoma, to confirm the diagnosis, to control the effect of the treatment, and to detect recurrent disease. Serum NSE determination should not be used for cancer screening.

Radiometric immunoassay (IRMA) is used in NSE assessment [3]. This is a monoclonal two-site single incubation inmunoradiometric (sandwich) assay. The sample is incubated with plastic beads coated with antibody to NSE and an antibody against NSE, labelled with ^{125}I. The antibodies bind to different epitopes of the NSE molecule, whereby the labelled antibody is indirectly bound to the beads. After washing the unreacted radioactive antibody off the bead, the radioactivity bound to the bead is measured using a gamma counter.

Kinetics and equilibrium in antigen-antibody reactions are determining factors in the sensitiveness and accuracy of immunoanalytical techniques [4–6]. In previous research [1,2,7–9], different characteristics have been studied in relation with the antigen-antibody reactions used in analytical techniques that employ radioactivity as a measurable magnitude. The results suggest diffusive control in this type of processes. Stenberg et al. [10–13] proposed an application model for reactions occurring in the solid–liquid interphase and provided an equation with four parameters that indicated diffusion influence.

Equilibrium data analysis is used to a great extent in determining the capacity of a substance to bind to one or several receptor populations. Nonetheless, as pointed out by Weber [14], detecting two binding sites through such an assay requires the ligand to have very different affinity for the two binding sites.

Xavier and Wilson [15,16] studied the association and dissociation reactions of Hen Egg Lysozime (HEL) with two of its specific antibodies (HyHEL-5 and HyHEL-10) under pseudo first order conditions for the association, and found diffusion control. The decrease in the reaction rate constants as a result of viscosity turned out to be more drastic than theoretically expected, this aspect being put down to potential osmotic effects. In addition, rate constants were found to approximately double when ionic strength goes down from 500 to 27 mM, which indicates that the process occurs between species with opposite charges that affect the orientational requirements of association.

A diffusion-controlled process should meet some standard requirements such as a considerable reaction rate decrease when medium viscosity is greater, and slight temperature influence with a reduced energy demand with regard to activation, this causing activation enthalpy values to be of the same order as the solvent's viscous flow energy (5000 cal/mol for water).

Our research is aimed at applying a previously described kinetic model [1,2] to the reaction between NSE and its specific antibodies. Such a model should be able to account for the influence of the concentration of the reagents for both the global reaction and its stages, as well as the effect of temperature. As a complementary factor, the influence of viscosity on such processes is analysed. The media have different dielectric constants which—should the reaction occur between charged species—would give way to an effect that would overlap with that of viscosity. In order to indirectly estimate this potential influence, reactions are studied in media with different ionic strength.

The ultimate goal is to distinguish between single-site and two-site binding models by analysing kinetic data, as proposed by Motulsky and Mahan [17] and later by Karlsson and Neil [18]. These authors noticed that the distinction between single-site binding and two-site binding models was in many cases impossible through equilibrium analysis, while at the same time it was indeed feasible on the basis of kinetic experiments. The latter authors proposed a method which was applied to the study of the binding of titriade Noscapine (antitussive) to guinea pig brain homogenate which can have a general application for single and double site binding model receptor populations with ligand excess. This would allow for the discrimination between binding models and the study of binding parameters by using kinetic data only.

2. Material and methods

2.1. Reagents

1) Dry beads coated with monoclonal anti-NSE antibodies.
2) Solution of ^{125}I labelled monoclonal anti NSE antibodies (Tracer).
3) NSE standard solutions. Vials containing lyophilized NSE material. These were reconstructed with distilled water. Reagent 2 and 3 contain $<0.1\%$ sodium azide as a preservative.

All the reagents used were included in the NSE immunoradiomtric assay kit Proligen® NSE IRMA manufactured by Sangtec Medical.

2.2. Instruments

LKB Gammamaster Automatic Gamma Counter. Brookfield DV–II digital viscosimeter. Viscosity measurements were performed at 60 rpm with a UL ADADPTER . Beads washing systems.

2.3. Experimental procedure

Reaction kinetics were studied by placing the standards, the solution of ^{125}I labelled monoclonal anti NSE antibodies, and the coated beads in the polystyrene tubes and letting them react at different times: 0, 15, 30, 60 and 120 min and at 24 h, this being considered infinite time. Once the reaction time elapsed, radioactivity was measured for each tube by the gamma counter. Experiments were performed at 20 °C except for those relative to temperature influence.

Twenty five experiments were performed, arranged as follows:

2.3.1. Experiments 1–7

Study of the influence of NSE (Q) and tracer (M) concentrations upon the global reaction. 25 μl of Q and 200 μl of M from different concentrations were left to react.

2.3.2. Experiments 8–10

Study of the influence of the concentrations of the previously mentioned factors upon the first process stage, i.e. upon the binding of Q to the antibody bound to the bead (P). Q-coated beads were incubated at different times; later on and once washed, M was added and it was left to react for 24 h.

2.3.3. Experiments 11–13

Study of the influence of the same factors upon the second process stage, namely the biding of M to the PQ immunocomplex. Beads and Q were left to react for 24 h and, once washed, M was added and it was left to react at different times.

2.3.4. Experiments 14–17

Study of the influence of temperature. Four experiments were carried out at constant Q and at four different temperatures.

2.3.5. Experiments 18–21

Study of the influence of viscosity at Q and M constant concentrations using four solutions prepared as per the table below (quantities in ml). In the experiments, 200 μl of the solutions were taken and left to react with 25 μl of Q. Final viscosity of the solutions obtained in this manner was determined by comparison with a calibration curve drawn from standard glycerol–water mixes.

FINAL η (mPa · s)	1.368	1.470	1.610	1.815
GLYCEROL	0.0	0.2	0.4	0.6
DISTILLED H_2O	1.8	1.6	1.4	1.2
TRACER	1.0	1.0	1.0	1.0

2.3.6. Experiments 22–25

Study of the influence of ionic strength at Q and M constant concentrations, using four solutions prepared as per the table below (quantities in ml). In the experiments, 200 μl of the solutions were taken and left to react with 25 μl of Q. Final ionic strength of the reacting mixes obtained in this manner are shown in the table.

FINAL I (mol l^{-1})	0.026	0.052	0.078	0.104
ClNa 0.410 M	0.2	0.4	0.6	0.8
DISTILLED H_2O	1.6	1.4	1.2	1.0
TRACER	1.0	1.0	1.0	1.0

Table 1
Influence of M and Q concentrations (global reaction)

t (min)	0	15	30	60	90	120	∞	v_0	M	Q
Z_1	722.0	5019.0	8728.3	11112.0	15397.4	17034.1	53092.7	306.6 (r = 0.994)	100	166.6
Z_2	568.9	3752.5	6374.6	8815.5	13256.0	14520.8	46369.3	193.9 (r = 0.994)	75	166.6
Z_3	238.6	2778.9	4771.2	6485.8	9084.7	10083.9	32759.0	171.0 (r = 0.996)	50	166.6
Z_4	205.0	1548.1	2509.8	3535.7	5249.3	5805.3	20409.9	75.6 (r = 0.995)	25	166.6
Z_5	226.1	393.1	659.0	878.0	1265.5	1372.1	2815.6	12.1 (r = 0.995)	100	6
Z_6	331.6	1260.4	1768.4	2357.6	2808.7	3005.5	7631.5	62.5 (r = 0.998)	100	20
Z_7	750.3	2936.7	3548.7	5992.5	6067.8	6592.7	21979.0	140.4 (r = 0.991)	100	60

Globally, the values fit with the equation:

$$Z = \frac{a_2 \cdot M_0 \cdot Q_0}{M_0 + b_2} \cdot \{1 - \exp(-t \cdot c_2 \cdot (M_0 + b_2))\} + d_2 \quad \text{(Identical to Eq. (2))}$$

a_2	b_2	c_2	d_2	r	s	AIC
792	147	1.026×10^{-5}	1099	0.997	34.0×10^6	858

Or with:

$$Z = \frac{a_3 \cdot M_0 \cdot Q_0}{M_0 + b_3} \cdot \{1 - \exp(-t \cdot c_3 \cdot (M_0 + b_3))\} + \frac{d_3 \cdot M_0 \cdot Q_0}{M_0 + e_3} \cdot \{1 - \exp(-t \cdot f_3 \cdot (M_0 + e_3))\} + g_3 \quad \text{(Identical to Eq. (3))}$$

a_3	b_3	c_3	d_3	e_3	f_3	g_3	r	s	AIC
566	88.3	8.75×10^{-5}	102.9	113.9	14.07×10^{-5}	758	0.998	17.7×10^6	832

2.4. Data analysis

The Statistica programme was used with specific non-linear regression equations. As the statistical criterion that allows a choice from different equations, AIC was observed (Akaike's Information Criterion), expressed as $\mathrm{AIC} = N \ln S + 2P$ where N is the number of points, S the addition of residual squares, and P the number of parameters in the equation. The fitting with the lowest AIC must be chosen.

2.5. Symbols

P	antibody bound to the bead
Q	NSE
M	^{125}I-labelled anti-NSE antibody
PQ	immunocomplex made of the antibody bound to the bead with the NSE
PQM	sandwich-type radioactive immunocomplex
$[P]$, $[Q]$, $[M]$, $[PQ]$, $[PM]$	mol/l concentrations
P_0, M_0, Q_0	initial concentrations in arbitrary units
Z	Cpm activity measured in each tube after reaction ($Z = Z_{sp} + Z_0$). A sub-index is added in the tables indicating the experiment number
Z_{sp}	activity specifically bound to the bead wall, directly proportional to the radioactive immunocomplex concentration

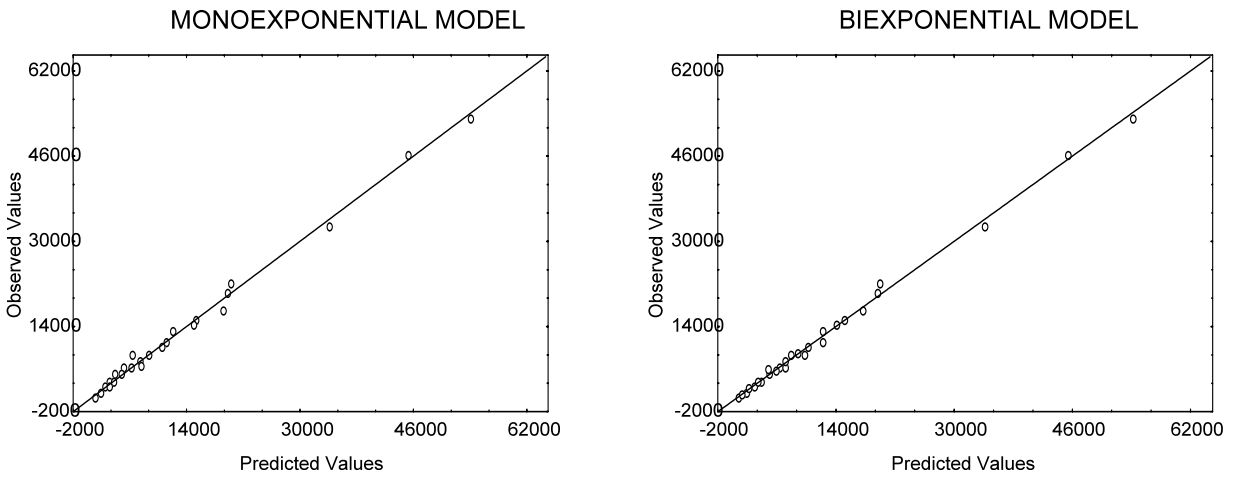

Fig. 1. Z values observed in experiments 1–7 (Table 1) vs. values predicted for Eqs. (2) and (3). Monoexponential model: Observed values $= -0.1904 + 1.0000 \cdot$ Predicted values, $r = 0.996$. Biexponential model: Observed values $= -0.00200 + 1.0000 \cdot$ Predicted values, $r = 0.997$.

Table 2
Influence of M and Q concentrations (stages)

t (min)	0	15	30	60	90	120	∞	v_0	M	Q
Stage 1										
Z_8	6488.1	18 909.5	24 228.2	27 092.9	30 633.6	35 633.2	52 023.0	873.3 ($r = 0.995$)	100	166.6
Z_9	4347.8	14 412.1	17 210.4	23 162.9	2466.0	25 571.0	34 768.6	432.8 ($r = 0.990$)	50	166.6
Z_{10}	1942.8	5445.9	7489.0	8177.5	8952.1	9485.2	10 008.9	263.9 ($r = 0.994$)	100	20
Stage 2										
Z_{11}	2990.0	8304.5	12 246.9	15 120.8	18 107.0	20 157.6	51 463.3	401.6 ($r = 0.998$)	100	166.6
Z_{12}	1891.0	4650.4	6618.6	9042.5	10 412.5	11 748.1	30 105.6	208.0 ($r = 1.000$)	50	166.6
Z_{13}	1652.3	2589.2	3254.1	4005.2	4520.2	5004.3	8625.3	70.1 (r = 1.000)	100	20

Z_0	value of Z obtained at $t = 0$. Corresponds to unspecific binding
Z_∞	value of Z obtained at t infinity
Z_e	value of Z_{sp} at equilibrium ($Z_e = Z_\infty - Z_0$)
t	time, min
T	temperature, K
v_0	initial rate
k	rate constant
K	equilibrium constant
η	viscosity (m Pa · s)
I	ionic strength (mol/l)
z	charge of chemical species
z	charge of chemical species
r	correlation coefficient
s	addition of residual squares

3. Results and discussion

3.1. Influence of M and Q concentration. Global reaction. (Experiments 1–7, Table 1) and stages (Experiments 8–13, Table 2)

This is the global process:

$$P + Q + M \rightarrow PQM$$

It can be broken down as follows:

Table 3
Influence of temperature ($Q = 166.6$ ng/ml)

t (min)	0	15	30	60	90	120	∞	v_0	T
Z_{14}	618.5	5054.5	7333.5	10 268.0	12 784.9	15 261.8	36 341.5	300.3 ($r = 0.999$)	278
Z_{15}	1009.2	5016.6	7548.7	12 779.5	16 413.0	18 835.9	43 140.6	253.2 ($r = 1.000$)	286
Z_{16}	722.0	5019.0	8728.5	11 112.0	15 397.4	17 034.1	53 092.7	306.6 ($r = 0.994$)	295
Z_{17}	1039.5	6171.9	8427.9	13 055.5	15 915.5	20 234.6	54 863.5	343.1 (r = 0.995)	300

Globally, the values fit with the equation:

$$Z = a_4 \cdot \{1 - \exp[-t \cdot b_4 \cdot T(\exp(\frac{-c_4}{T}))]\} + d_4 \quad \text{(Identical to Eq. (4))}$$

a_4	b_4	c_4	d_4	r	s	AIC
44 836	6.304×10^{-4}	1140	2525	0.978	249×10^6	549

Or with:

$$Z = a_5 \cdot \{1 - \exp[-t \cdot b_5 \cdot T(\exp(\frac{-c_5}{T}))]\} + d_5 \cdot \{1 - \exp[-t \cdot e_5 \cdot T(\exp(\frac{-f_5}{T}))]\} + g_5 \quad \text{(Identical to Eq. (5))}$$

a_5	b_5	c_5	d_5	e_5	f_5	g_5	r	s	AIC
51 400	0.967	3750	13 980	1.408×10^{-5}	−413	1153	0.998	22.2×10^6	488

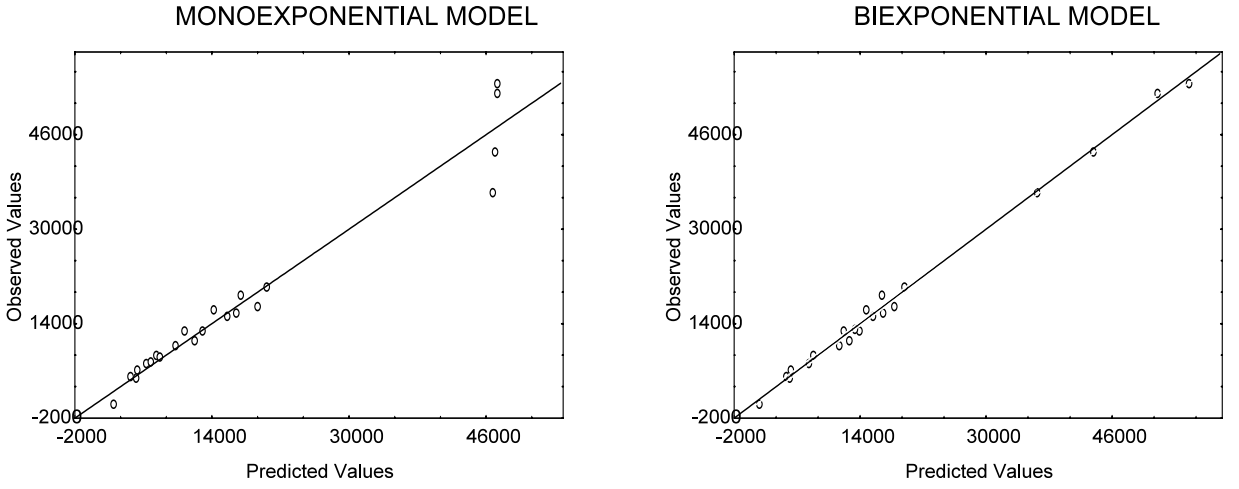

Fig. 2. Z values observed in experiments 8–13 (Table 3) vs. values predicted for Eqs. (4) and (5). Monoexponential model: Observed values = 0.0001 + 1.0000 · Predicted values. $r = 0.978$. Biexponential model: Observed values = −0.1224 + 1.0000 · Predicted values, $r = 0.998$.

Table 4
Influence of viscosity ($Q = 116$ ng/ml)

t (min)	0	15	30	60	90	120	∞	v_0	η
Z_{18}	302.5	3248.5	5218.6	6996.9	8319.6	9730.6	25 163.6	223.0 ($r = 0.995$)	1.368
Z_{19}	295.9	2835.0	4430.1	6261.0	7215.5	9014.8	23 956.3	196.6 ($r = 1.000$)	1.470
Z_{20}	71.1	2098.0	3739.7	5457.3	6279.8	8134.1	23 319.5	173.5 ($r = 1.000$)	1.610
Z_{21}	128.0	1917.2	3340.2	4670.8	5670.8	7054.1	22 477.8	145.8 ($r = 1.000$)	1.815

Globally, the values fit with the equation:

$$Z = a_6 \cdot \{1 - \exp(-t \cdot \frac{b_6}{\eta + c_6})\} + d_6 \quad \text{(Identical to Eq. (6))}$$

a_6	b_6	c_6	d_6	r	s	AIC
22 900	0.00249	−0.798	1157	0.996	11.7×10^6	464

Or with:

$$Z = a_7 \cdot \{1 - \exp(-t \cdot \frac{b_7}{\eta + c_7})\} + d_7 \cdot \{1 - \exp(-t \cdot \frac{e_7}{\eta + f_7})\} + g_7 \quad \text{(Identical to Eq. (7))}$$

a_7	b_7	c_7	d_7	e_7	f_7	g_7	r	s	AIC
21 500	0.001286	−0.912	3360	0.0211	−1.091	202	1.000	1.359×10^6	409

$$P + Q \underset{k_{-1}}{\overset{k_1}{\Leftrightarrow}} PQ \text{ (quick)}$$

$$\text{and} \quad PQ + M \underset{k_{-2}}{\overset{k_2}{\Leftrightarrow}} PQM \text{ (slow)}$$

The second stage is slower, as can be seen in Table 2. If it is assumed that quick equilibrium is reached, then:

$$\frac{[PQ]}{[P] \cdot [Q]} = \frac{k_1'}{k_{-1}} \qquad [PQ] = \frac{[P] \cdot [Q]}{[Q] + \frac{k_{-1}}{k_1'}}$$

Likewise, once equilibrium is reached, the following is applicable to the second one:

$$\frac{[PQM]}{[PQ] \cdot [M]} = \frac{k_2'}{k_{-2}} \qquad [PQM] = \frac{[PQ] \cdot [M]}{[M] + \frac{k_{-2}}{k_2'}}$$

from which we get:

$$[PQM] = \frac{[P] \cdot [Q] \cdot [M]}{\left([Q] + \frac{k_{-1}}{k_1'}\right) + \left([M] + \frac{k_{-2}}{k_2'}\right)} \qquad (01)$$

The rate of the second stage is:

$$\frac{\mathrm{d}[PQM]}{\mathrm{d}t} = k_2' \cdot [PQ] \cdot [M] \cdot k_{-2} \cdot [PQM] \qquad (02)$$

The experimental data encompasses activities as an indirect concentration measurement. By applying suitable transformations, Eqs. (01) and (02) become:

$$Ze = \frac{P_0 \cdot Q_0 \cdot M_0}{\left(Q_0 + \frac{m}{k_1}\right) \cdot \left(M_0 + \frac{n}{k_2}\right)} \qquad (03)$$

$$\frac{\mathrm{d}Z_{sp}}{\mathrm{d}t} = k_2 \cdot (Q_0 - Z_{sp}) \cdot (M_0 - Z_{sp}) - k_{-2} \cdot Z_{sp} \qquad (04)$$

The previous treatment implicitly acknowledges that $[Q] << [PQ] + [PQM]$.

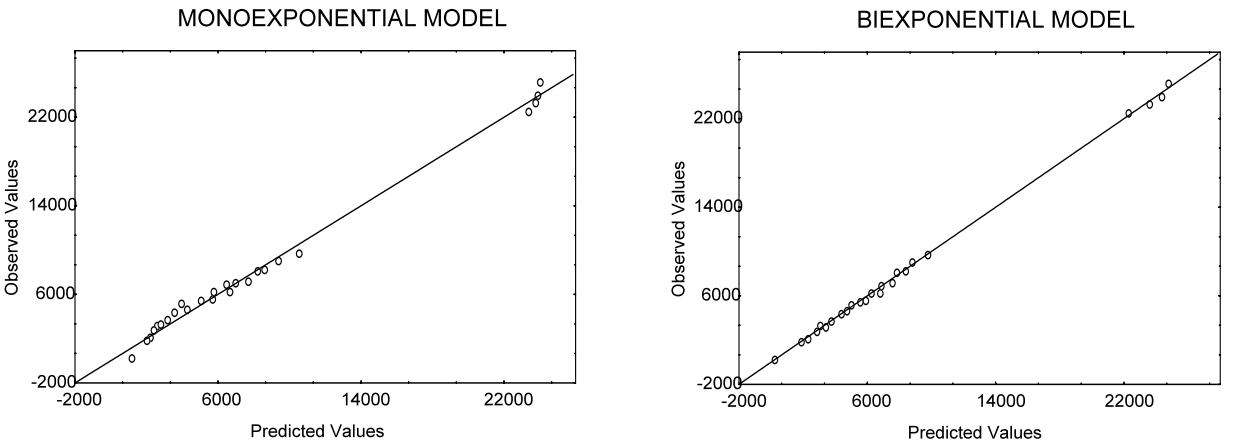

Fig. 3. Z values observed in experiments 18–21 (Table 4) vs. values predicted for Eqs. (6) and (7). Monoexponential model: Observed values = $-0.2049+1.0000 \cdot$ Predicted values, $r=0.996$. Biexponential model: Observed values = $0.00106+1.0000 \cdot$ Predicted values. $r=1.0000$.

The integration of (Eq. (04)) provides the following:

$$Z=\frac{P_0 \cdot Q_0 \cdot M_0}{\left(Q_0+\frac{m}{k_1}\right)\cdot\left(M_0+\frac{n}{k2}\right)}\cdot\frac{1-\exp\{-((Q_0+M_0-2Ze)\cdot k_2+k_{-2})\cdot t\}}{1-\frac{Ze^2}{Q_0\cdot M_0}\cdot\exp\{-((Q_0+M_0-2Ze)\cdot k_2+k_{-2})\cdot t\}}+Z_0$$

which, taking Eq. (03) into account, becomes:
which can be reduced to:

$$Z=\frac{Ze\cdot\{1-\exp(-(Q_0+M_0-2Ze)\cdot k_2+k_{-2})\cdot t\}}{1-\left(\frac{Ze^2}{Q_0\cdot M_0}\right)\cdot\exp\{-((Q_0+M_0-2Ze)\cdot k_2+k_{-2})\cdot t\}}+Z_0$$

$$Z=\frac{P_0\cdot Q_0\cdot M_0}{\left(Q_0+\frac{m}{k_1}\right)\cdot\left(M_0+\frac{n}{k_2}\right)}\cdot\{1-\exp[-((Q_0+M_0-2Ze)k_2+k_{-2})\cdot t]\}+Z_0 \quad (1)$$

Eq. (1) was deduced in a previous paper [8]:

If in Eq. (1) the approximation $Ze=j\cdot Q_0$ is carried out (valid if $P_0>>M_0>>Q_0$), then after simplification we have:

$$Z=\frac{a_2\cdot M_0\cdot Q_0}{M_0+b_2}\cdot\{1-\exp(-t\cdot c_2\cdot(M_0+b_2))\}+d_2 \quad (2)$$

(Mono-exponential equation)

Table 5
Influence of ionic strength ($Q = 100$ ng/ml)

t (min)	0	15	30	60	90	120	∞	v_0	I
Z_{22}	320.5	3137.0	3987.1	5250.6	6942.2	8875.0	21 957.2	171.3 ($r = 0.995$)	0.026
Z_{23}	350.3	2660.1	3558.0	4950.5	6311.0	7044.4	22 225.2	138.8 ($r = 0.996$)	0.052
Z_{24}	146.3	1994.9	3076.5	4224.6	5675.3	6939.5	20 680.5	124.8 ($r = 0.998$)	0.078
Z_{25}	221.5	1742.4	2368.1	3291.7	4172.8	5406.6	17 247.0	100.7 ($r = 0.998$)	1.104

Globally, the values fit with the equation:
$Z = a_8 \cdot \exp(b_8 \cdot I^{1/2}) \cdot \{1 - \exp(-c_8 \cdot t \cdot \exp(d_8 \cdot I^{1/2}))\} + e_8$ (Identical to Eq. (8))

a_8	b_8	c_8	d_8	e_8	r	s	AIC
26 381	−1.1668	0.00594	−2.65	988	0.995	11.2×10^6	464

Or with:
$Z = a_9 \cdot \exp(b_9 \cdot I^{1/2}) \cdot \{1 - \exp(-c_9 \cdot t \cdot \exp(d_9 \cdot I^{1/2}))\} + e_9 \cdot \exp(f_9 \cdot I^{1/2}) \cdot \{1 - \exp(-g_9 \cdot t \cdot \exp(h_9 \cdot I^{1/2}))\} + j_9$ (Identical to Eq. (9))

a_9	b_9	c_9	d_9	e_9	f_9	g_9	h_9	j_9	r	s	AIC
14 934	1.739	0.2435	−12.71	687	6.622	5.59	−19.94	365	0.999	2.35×10^6	429

And for two binding sites, we have:

$$Z = \frac{a_3 \cdot M_0 \cdot Q_0}{M_0 + b_3} \cdot \{1 - \exp(-t \cdot c_3 \cdot (M_0 + b_3))\} + \frac{d_3 \cdot M_0 \cdot Q_0}{M_0 + e_3} \cdot \{1 - \exp(-t \cdot f_3 \cdot (M_0 + g_3))\} + n_3 \quad (3)$$

(Bi-exponential equation)

The results obtained in the global reaction for different M and Q concentrations were studied in experiments 1–7 whose results and correlation equations are shown in Table 1, Fig. 1.

Please note that the fitting is better for Eq. (3) than for Eq. (2), which shows that results are better interpreted if a two-site binding model is admitted.

The results of the two stages in which the global reaction can be divided were studied in experiments 8–13, whose results are shown in Table 2.

Stage 2 is the slowest and so limits the process rate.

3.2. Influence of temperature (Experiments 14–17, Table 3)

If rate and equilibrium constants (c_2, c_3, f_3–b_2, b_3, e_3, respectively) are written on Eqs. (2) and (3) as per Eyring and van t'Hoff and then simplified, then:

$$Z = a_4 \cdot \left\{1 - \exp\left[-t \cdot b_4 \cdot T\left(\exp\left(\frac{-c_4}{T}\right)\right)\right]\right\} + d_4 \quad (4)$$

$$Z = a_5 \cdot \left\{1 - \exp\left[-t \cdot b_5 \cdot T\left(\exp\left(\frac{-c_5}{T}\right)\right)\right]\right\} + d_5 \cdot \left\{1 - \exp\left[-t \cdot e_5 \cdot T\left(\exp\left(\frac{-f_5}{T}\right)\right)\right]\right\} + g_5 \quad (5)$$

This was studied in experiments 14–17, whose results and correlation equations are shown in Table 3, Fig. 2.

The activation enthalpy for the process is $\Delta H = R \cdot m = 2 \cdot 3609 = 7218$ cal/mol, its magnitude

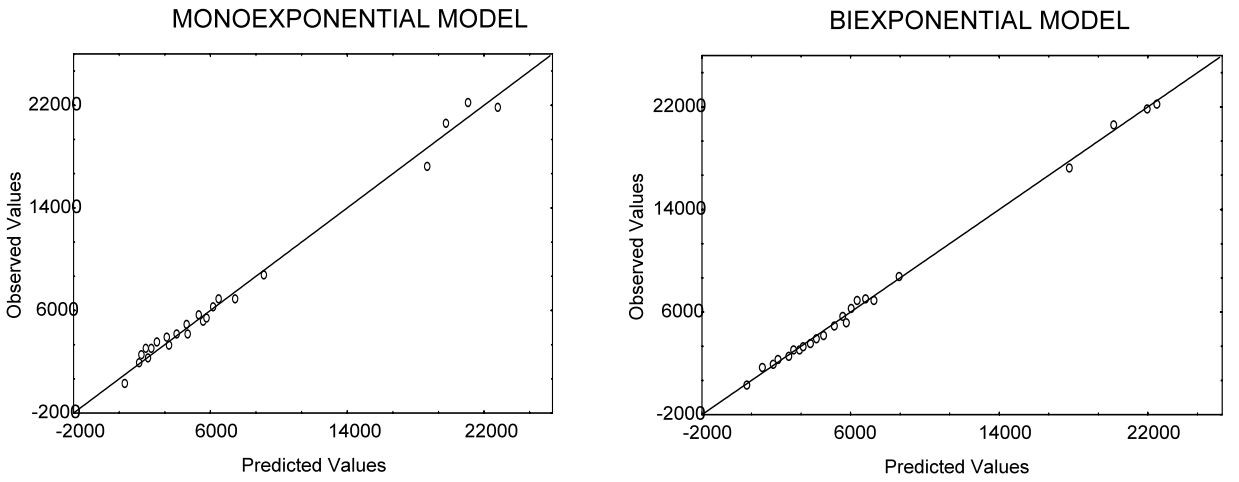

Fig. 4. Z values observed in experiments 22–25 (Table 5) vs. values predicted for Eqs. (8) and (9). Monoexponential model: Observed values $= -0.00012 + 1.0000 \cdot$ Predicted values, $r = 0.995$. Biexponential model: Observed values $= -0.0083 + 1.0000 \cdot$ Predicted values, $r = 0.999$.

Table 6
Comparative mono and bi-exponential

	M and Q concentration	Temperature	Viscosity	Ionic strength
Mono-exponential	$r = 0.997$	$r = 0.978$	$r = 0.996$	$r = 0.995$
	$s = 34.0 \times 10^6$	$s = 249 \times 10^6$	$s = 11.7 \times 10^6$	$s = 11.2 \times 10^6$
	AIC = 858	AIC = 549	AIC = 464	AIC = 464
Bi-exponential	$r = 0.998$	$r = 0.998$	$r = 1.000$	$r = 0.999$
	$s = 17.7 \times 10^6$	$s = 22.2 \times 10^6$	$s = 1.36 \times 10^6$	$s = 2.35 \times 10^6$
	AIC = 832	AIC = 488	AIC = 409	AIC = 429

order being that of the viscous flow energy of water.

3.3. Influence of Viscosity. (Experiments 18–21, Table 4)

Kramers [19] pointed out that rate constants k^0 and k^v obtained in the absence and presence of a viscosizing agent such as glycerol relate to the corresponding viscosities through the equation

$$\frac{k^0}{k^V} = A + B \cdot \frac{\eta}{\eta_0}$$

Finding the value of k^v in the previous equation, substituting it in lieu of k_1 and k_2 in Eqs. (2) and (3), and simplifying, we then have:

$$Z = a_6 \cdot \left\{1 - \exp\left(-t \cdot \frac{b_6}{\eta + c_6}\right)\right\} + d_6 \tag{6}$$

$$Z = a_7 \cdot \left\{1 - \exp\left(-t \cdot \frac{b_7}{\eta + c_7}\right)\right\} + d_7 \cdot \left\{1 - \exp\left(-t \cdot \frac{e_7}{\eta + f_7}\right)\right\} + g_7 \tag{7}$$

This was studied in experiments 18–21, whose results and correlation equations are shown in Table 4, Fig. 3.

Please note that Z values for all times and for equilibrium fall as viscosity increases.

3.4. Influence of ionic strength (Experiments 22–25, Table 5)

The results are quantitatively justified by introducing the Debye–Hückel equation into Eqs. (2) and (3):

$$k = k_0 \quad \exp(2.344 \cdot z_0 \cdot z_u \cdot I^{1/2})$$

for terms d_8, d_9, h_9, corresponding to rate constants, and b_8, b_9, f_9 representing equilibrium ones. By putting the constants together and simplifying, then we have:

$$Z = a_8 \cdot \exp(b_8 \cdot I^{1/2}) \cdot \{1 - \exp(-c_8 \cdot t \cdot \exp(d_8 \cdot I^{1/2}))\} + e_8 \quad (8)$$

$$Z = a_9 \cdot \exp(b_9 \cdot I^{1/2}) \cdot \{1 - \exp(-c_9 \cdot t \cdot \exp(d_9 \cdot I^{1/2}))\} + e_9 \cdot \exp(f_9 \cdot I^{1/2}) \cdot \{1 - \exp(-g_9 \cdot t \cdot \exp(h_9 \cdot I^{1/2}))\} + j_9 \quad (9)$$

This was studied in experiments 22–25, whose results and correlation equations are shown in Table 5, Fig. 4.

The reaction is slower as ionic strength rises. Parameters c''' and e''' contain the product of the charges of the reagents, their values indicating that the reaction takes place between species with small charges and opposite signs.

4. Conclusion

As shown by Table 6 and Figs. 1–4, the bi-exponential model fits better than the mono-exponential one as far as the obtained results are concerned, this justifying the influence of Q and M concentrations, temperature, viscosity, and ionic strength. Therefore, we can draw the conclusion that experimental results are better explained by admitting that two different processes occur—corresponding to the two-site binding reactions—in the interaction between NSE and its antibody immobilised on a spherical surface.

References

[1] J. García Gómez, M. Porcar Pons, J.L. Moreno Frigols, J. Pharm. Biomed. Anal. 29 (2002) 307–315.
[2] J. García Gómez, J.L. Moreno Frigols, J. Immunoassay Immunochem. 23 (2002) 347–367.
[3] L.E.M. Miles, C.N. Hales, Immunoradiometric assay procedures: new developments, in: In Vitro Procedures with Radioisotopes in Medicine, Vienna, 1970, pp. 483–484.
[4] E. Zuber, G. Mathis, J.P. Flandrois, Anal. Biochem. 251 (1997) 79–88.
[5] E. Zuber, et al., J. Immunoassay 18 (1997) 21–47.
[6] S.Y. Rabbany, et al., Anal. Lett. 31 (1998) 1663–1675.
[7] C. Olivas Arroyo, J.L. Moreno Frigols, J. Pharm. Biomed. Anal. 26 (2001) 547–562.
[8] C. Olivas Arroyo, M.J. Duart Duart, J.L. Moreno Frigols, J. Immunoassay Immunochem. 23 (2002) 407–428.
[9] M.J. Duart Duart, C. Olivas Arroyo, J. L. Moreno Frigols, Clin. Chem Lab. Med. 40 (2002) 1161–1167.
[10] M. Stenberg, L.L. Stiblert, J. Theor. Biol. 120 (1986) 129–140.
[11] H. Nygren, M. Werthen, M. Stenberg, J. Immunol. Methods 101 (1988) 63–71.
[12] H. Nygren, M. Stenberg, Immunology 66 (1989) 321–327.
[13] M. Stenberg, H. Nygren, J. Immunol. Methods 113 (1988) 3–15.
[14] G. Weber, The binding of small molecules to proteins, in: B. Pullman, M. Weissblut (Eds.), Molecular Biophysic, Academic Press, New York, 1965, p. 369.
[15] K.A. Xavier, R.C. Willson, Biophys. J. 74 (1998) 2036–2045.
[16] K.A. Xavier, S.M. McDonald, J.A. McCammon, R.C. Willson, Protein Eng. 12 (1999) 79–83.
[17] H.J. Motulsky, L.C. Mahan, Mol. Pharmacol. 25 (1984) 1–9.
[18] M. Karlsson, A. Neil, Eur. J. Pharmacol. 148 (1988) 115–125.
[19] H.A. Kramers, Physica 7 (1940) 284–304.